Chapter -8

Indian Ocean Dipole influence on Indian summer monsoon and ENSO: A review

Annalisa Cherchi[1], Pascal Terray[2], Satyaban B. Ratna[3], Syam Sankar[4], Sooraj KP[5], Swadhin Behera[6]

[1]Institute of Atmospheric Sciences and Climate (ISAC-CNR), Bologna, Italy

[2]LOCEAN/IPSL, Sorbonne Universités (UPMC, Univ Paris 06)-CNRS-IRD-MNHN, Paris, France

[3]Climatic Research Unit, School of Environmental Sciences, University of East Anglia, Norwich, NR4 7TJ, United Kingdom

[4]Advanced Centre for Atmospheric Radar Research (ACARR), Cochin University of Science and Technology, Kochi, India

[5]Centre for Climate Change Research, Indian Institute of Tropical Meteorology, Ministry of Earth Sciences (IITM-MoES), Pune 411008, India

[6]Application Laboratory, Research Institute for Value-Added-Information Generation, Japan Agency for Marine-Earth Science and Technology, Yokohama, Japan

Corresponding author:

Annalisa Cherchi (ISAC-CNR)

E-mail: a.cherchi@isac.cnr.it

Abstract

The Indian Ocean Dipole (IOD) is one of the dominant modes of variability of the tropical Indian Ocean and it has been suggested to have a crucial role in the teleconnection between the Indian summer monsoon and El Niño Southern Oscillation (ENSO). The main ideas at the base of the influence of the IOD on the ENSO-monsoon teleconnection include the possibility that it may strengthen summer rainfall over India, as well as the opposite, and also that it may produce a remote forcing on ENSO itself. In the future, the IOD is projected to increase in frequency and amplitude with mean conditions mimicking the characteristics of its positive phase. Still, state-of-the-art global climate models have large biases in representing mean state and variability of both IOD and ISM, with potential consequences for their future projections. However, the characteristics of the IOD and ENSO are likely to continue in a future warmer world, with a persistence of their linkage.

Keywords: Indian Ocean Dipole, Indian summer monsoon rainfall, ENSO, remote forcing, air-sea coupling, coupled climate models, biases, projections

8.1 Introduction

The Indian summer monsoon (ISM) is one of the main components of the South Asian summer monsoon, representing the largest source of moisture and precipitation over the tropical sector (Webster et al., 1998). The ISM is highly variable and its variability is partly modulated by external factors, the El Niño Southern Oscillation (ENSO) being one of the most important. The remote connection between ENSO and ISM is known since the beginning of the nineteenth century and it has been largely investigated in the past (Walker, 1924; Sikka, 1980; Rasmusson and Carpenter, 1983; Kirtman and Shukla, 2000, among others). Schematically, during warm ENSO episodes the rising limb of the Walker circulation over West Pacific shifts eastward in response to a warming of the eastern Pacific, causing descent of air to the west of it and aiding decreased monsoon rainfall over India (Goswami, 1998; Lau and Wang, 2006). It has been natural also to explore the possible influence of the neighboring Indian Ocean on the ISM variability, with many studies pointing out significant connections (Rao and Goswami, 1988; Ashok et al., 2001, 2004; Gadgil et al., 2004, 2005, 2007; Krishnan et al., 2003; Terray et al., 2005, 2007; Cherchi et al., 2007; Izumo et al., 2008; Boschat et al., 2011, 2012; Cherchi and Navarra, 2013; Shukla and Huang, 2016, among many others).

The Indian Ocean Dipole (IOD) was discovered at the end of the 90s (Saji et al., 1999; Webster et al., 1999) and it is recognized as one of the dominant modes of variability of the tropical Indian Ocean Sea Surface Temperature (SST). Toward the end of the 20th century, weakening in the strength of the ENSO-monsoon relationship have been documented (Kumar et al., 1999; Kinter et al., 2002) and, since its discovery, the IOD has been identified as one potential element that modulates the ENSO-monsoon connection (Ashok et al., 2001; Li et al., 2003). Contrasting literature about its active or passive role has been produced since then and the debate is still open (Ashok et al., 2001; Li et al., 2003; Meehl et al., 2003; Ashok et al., 2004; Wu and Kirtman, 2004; Cherchi et al., 2007; Krishnan et al., 2011; Cherchi and Navarra, 2013; Krishnaswamy et al., 2015; Chowdary et al., 2015; Srivastava et al., 2019, to mention a few).

This chapter intends to provide an updated review on the current understanding about the influence of the IOD on the ISM and its teleconnection with ENSO. In particular, the chapter is organized as follows: Section 8.2 is dedicated to the description of the IOD, while Section 8.3 is focused on the processes at work in IOD influencing the monsoon and its relationship with ENSO, also from a modelling point of view. Section 8.4 reviews the literature about past evidence, present case studies and future projections about the topic, and Section 8.5 is dedicated to the discussion of the results reviewed, highlighting some of the associated challenges and related future perspectives. Finally, Section 8.6 collects the main conclusion derived from the review.

8.2 Some salient features of the Indian Ocean Dipole

The IOD is characterized by a zonal dipole in the tropical Indian Ocean with positive SST anomalies in the western equatorial Indian Ocean (50°-70°E, 10°S-10°N) and negative SST anomalies toward Sumatra (90°-110°E, 10°S-EQ) in its positive phase (Fig. 8-1; Saji et al., 1999). The formation of the IOD relies on the Bjerknes feedback, requiring background surface easterlies and thermocline shallowing in the eastern part along the Equator (Fig. 8-1; Schott et al., 2009). These conditions set in boreal spring and persist until autumn, explaining the IOD development in boreal summer, its peak toward autumn and its rapid termination before winter, because of the monsoon wind swing (Schott et al., 2009).

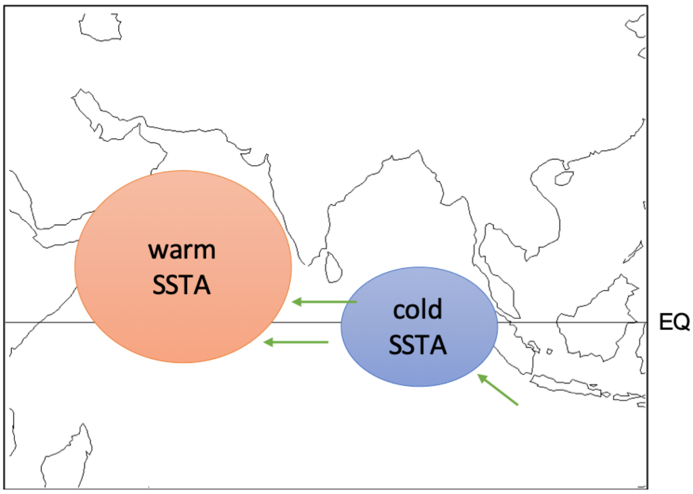

Fig. 8-1: Schematic of the Indian Ocean Dipole in its positive phase with warm SST anomalies on the west and cold SST anomalies toward the coast of Sumatra. The green arrows indicate the direction of the prevailing corresponding surface winds.

Before the discovery of the IOD as one of the dominant modes of variability of the tropical Indian Ocean, earliest suggestions of inherent coupled dynamics in the basin identified periods of anomalous easterlies in the central Indian Ocean concurrent with anomalous cold (warm) SST in the eastern (western) part, that occurred during boreal fall in the absence of ENSO (Reverdin et al., 1986). Significant feedback mechanisms at play between zonal SST and pressure gradient, equatorial easterly wind anomalies and precipitation anomalies in the western equatorial Indian Ocean were later identified (Hastenrath et al., 1993). An east-west seesaw in sea level anomaly in the tropical Indian Ocean was noticed and correlated with thermocline depth changes (Murtugudde et al., 1995). This east-west sea level dipole has been associated with the east-west SST gradient and strongly correlated with the Indian summer monsoon rainfall (Murtugudde et al., 1998). The SST gradient was shown to be in phase with equatorial zonal wind anomalies (Murtugudde and Busalacchi, 1999).

Since its discovery there has been strong debate and controversy whether the IOD is an intrinsic mode of Indian Ocean coupled variability, or whether and how it is driven by external forcing, like ENSO (e.g., Hastenrath, 2002; Dommenget and Latif, 2002; Yamagata et al., 2003; Murtugudde et al., 2003; Behera et al., 2003). Many studies claim that most of the IOD variability is driven by ENSO (Allan et al., 2001; Baquero-Bernal et al., 2002; Huang and Kinter, 2002; Dommenget, 2011; Zhao and Nigam, 2015; Zhao et al., 2019), while others suggest that IOD is a self-sustained mode of oscillation (Ashok et al., 2003; Yamagata et al., 2004; Behera et al., 2006). About 20% of the IOD events seem to co-occur with ENSO (Fig. 8-2; Saji, 2018). IOD events that could be categorized as with or without the influence of ENSO have systematic differences in their temporal evolution and spatial distribution, including periodicity, strength and formation processes (Behera et al., 2006; Hong et al., 2008). Modeling studies confirm that IOD events are often triggered by ENSO, but they also demonstrate that IOD events can exist without ENSO by means of dedicated sensitivity experiments in which ENSO is removed by different nudging techniques (Lau and Nath, 2004; Fischer et al., 2005; Behera et al., 2006; Wang et al., 2016; 2019; Cretat et al., 2017, 2018). In the absence of ENSO, the interannual IOD variability is mostly biennial (Behera et al., 2006; Cretat et al. 2018), while in years of co-occurrences ENSO affects the periodicity, strength, and formation processes of IODs (Cretat et al. 2018).

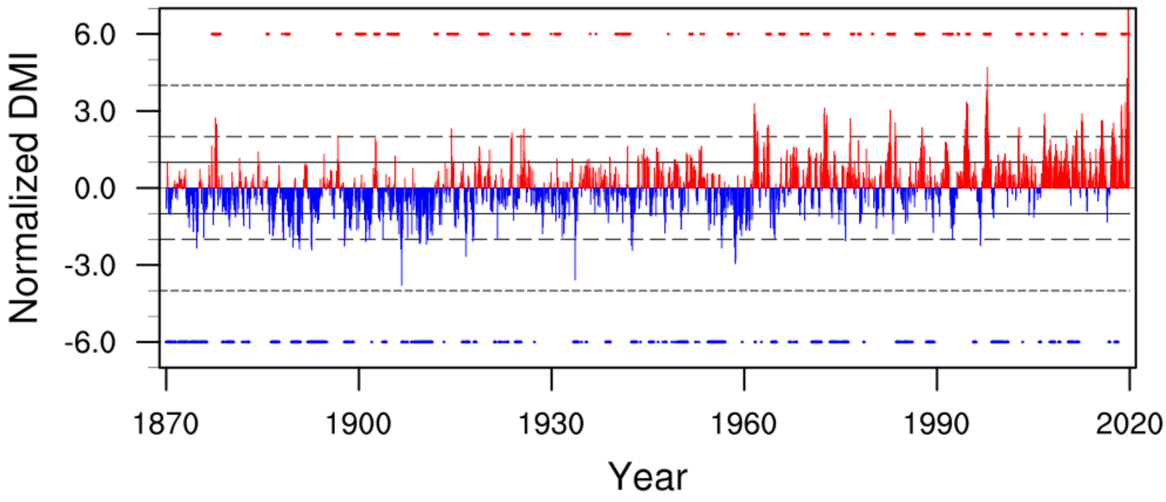

Fig. 8-2: Normalized monthly IOD index (Standard deviation) defined as anomalous SST gradient between the western equatorial Indian Ocean (50°E-70°E and 10°S-10°N) and the southeastern equatorial Indian Ocean (90°E-110°E and 10°S-0°N). Anomalies (with respect to 1981-2010 mean) have been downloaded from https://psl.noaa.gov/gcos_wgsp/Timeseries/DMI/, but 2019 values have been integrated from JAMSTEC repository (http://www.jamstec.go.jp/virtualearth/general/en/index.html). Red and blue markers along 6 and -6 std correspond to NINO3.4 anomalies (1981-2010 mean removed) larger than 0.5°C. NINO3.4 anomalies have been downloaded from https://psl.noaa.gov/gcos_wgsp/Timeseries/Nino34/. As indicated in the respective websites, both IOD and NINO3.4 values are computed from the HadISST1 dataset (Rayner et al., 2003).

Through changes in the atmospheric circulation, the IOD exerts its influence on, among others, the Southern Oscillation (Behera and Yamagata, 2003), the summer climate condition in Europe (Behera et al., 2012), East Asia (Guan and Yamagata, 2003; Guan et al., 2003; Chen et al., 2019) and streamflows in the western part of Indonesia (Sahu et al., 2012), as well as on rainfall over Africa (Black et al., 2003; Manatsa and Behera, 2013; Endris et al., 2019), Sri Lanka (Zubair et al., 2003), Australia (Ashok et al., 2003; Ummenhofer et al., 2013; Dey et al., 2019; Hossain et al., 2020), and Brazil (Chan et al., 2008; Taschetto and

Ambrizzi, 2012; Bazo et al., 2013). In the following we focus on the IOD influence on the summer monsoon rainfall over India and linkages with ENSO, which are both subject of important controversies in the literature.

8.3 IOD and the ENSO-monsoon teleconnections: processes at work

To influence the ISM and its ENSO teleconnection, IOD events should develop from boreal summer (June to August). As described by Schott et al. (2009), this is in fact the case for many IOD events. However, some IODs peak in the peak monsoon season (Du et al., 2013), though a few others develop later. According to that, strong interactions between IOD and ISM can be expected during boreal summer and the withdrawal phase of the monsoon.

Some authors suggested a direct influence of the IOD on the ISM rainfall (ISMR) through moisture transport over the western Indian Ocean or modifications of the local Hadley cell, with enhanced ascendance and a northward shift of its uplift branch during positive IOD events, both enhancing ISM rainfall (Fig. 8-3a; Ashok et al., 2001, 2004; Gadgil et al., 2004; Behera et al., 2005; Ashok and Saji, 2007; Behera and Ratman, 2018). Recent investigations also reveal that early IODs (i.e., peaking in July) or prolonged IODs (i.e., lasting longer, more than 8 months) have excess of evaporation from the Arabian Sea and stronger cross-equatorial flow, leading to enhanced monsoon activity with decreased numbers of break spells (Anil et al., 2016). Others suggest that positive IOD events during boreal fall normally follow weak ISMs, and vice versa, as ISM circulation during boreal summer can also induce an equatorial anomalous SST gradient in the Indian Ocean during the following boreal fall (Loschnigg et al., 2003, Meehl et al., 2003; Terray et al., 2005, 2007). In this framework, ENSO, ISM and IOD appear as strongly inter-related components of the Tropospheric Biennial Oscillation (TBO) in the tropics (Fig. 8-3b; Meehl and Arblaster, 2002; Meehl et al., 2003; Li et al., 2006; Drbohlav et al., 2007; Webster and

Hoyos, 2010). The development of the IOD during boreal summer and autumn can lead to SST warming in the tropical southwest Indian Ocean via ocean dynamics during the next boreal winter and spring (Xie et al., 2002; Chowdary and Gnanaseelan 2007; Du et al., 2009; Chowdary et al., 2009). This warming can further influence the ISM onset in the following year, especially for IOD events co-occurring with El Niño in the Pacific Ocean and followed by a basin-wide Indian Ocean warming (Annamalai et al., 2005; Yang et al. 2007; Hong et al. 2010).

The ISMR response is not necessarily spatially coherent to the IOD phases (Behera and Ratman, 2018). The anomalous moisture transports to India associated with a positive IOD strengthen the monsoon trough and rainfall through an intensified monsoon-Hadley circulation (Behera et al., 1999; Ashok et al., 2001; Anil et al., 2016), with below normal rainfall to the south and to the north of the trough. During positive IODs, the north–south precipitation (heating) gradient over the eastern Indian Ocean dominates over the one in the equatorial Indian Ocean, resulting in a regional meridional circulation with uplift over the monsoon trough and sinking in the eastern lobe (Annamalai et al., 2003). On the other hand, in a negative IOD event, a regional Walker circulation and the moisture distribution favor moisture divergence (convergence) in the eastern (western) part of India. This gives rise to a zonal dipole in the rainfall anomalies with abundant rainfall on the western part and scanty rainfall on the east. The resulted regional asymmetry is a unique feature associated with the ISMR response to IOD but it is not well simulated by coupled General Circulation Models (CGCMs), though regional model experiments with different physical parameterization schemes may provide few combinations able to realistically reproduce the asymmetric response to the two phases of the IOD (Behera and Ratman, 2018).

IOD can influence the ENSO-ISM relationship indirectly (Ashok et al., 2001; Behera and Yamagata, 2003; Cai et al., 2011; Weller and Cai, 2013), by modulating ENSO events in the tropical Pacific itself (Luo et al., 2010; Izumo et al., 2010; Cai et al., 2019). Considering IOD events as triggered by ENSO, they may counteract its simultaneous influence on ISM (Ashok et al., 2001, 2004; Ashok and Saji, 2007; Ummenhofer et al., 2011; Lau and Nath, 2003, 2012; Krishnaswamy et al., 2015). More recently IOD has been suggested as potential trigger of ENSO, adding more complexity to the emerging picture (Luo et al., 2010; Izumo et al., 2010; Zhou et al., 2015; Jourdain et al., 2016; Wieners et al., 2017a,b; Wang et al., 2019; Cai et al., 2019). In fact, the Indian Ocean (either IOD and Indian Ocean Basin-wide Warming) has a highly significant impact on both the variability and predictability of ENSO, as evidenced by de-coupled experiments using different coupled climate models (Luo et al., 2010; Izumo et al., 2010; Santoso et al., 2012; Terray et al., 2016; Kajtar et al., 2016; Wang et al., 2019). For example, IOD events co-occurring with ENSO may fasten its phase transition (Kug and Kang, 2006; Luo et al., 2010; Izumo et al., 2010; Kug and Ham, 2012).

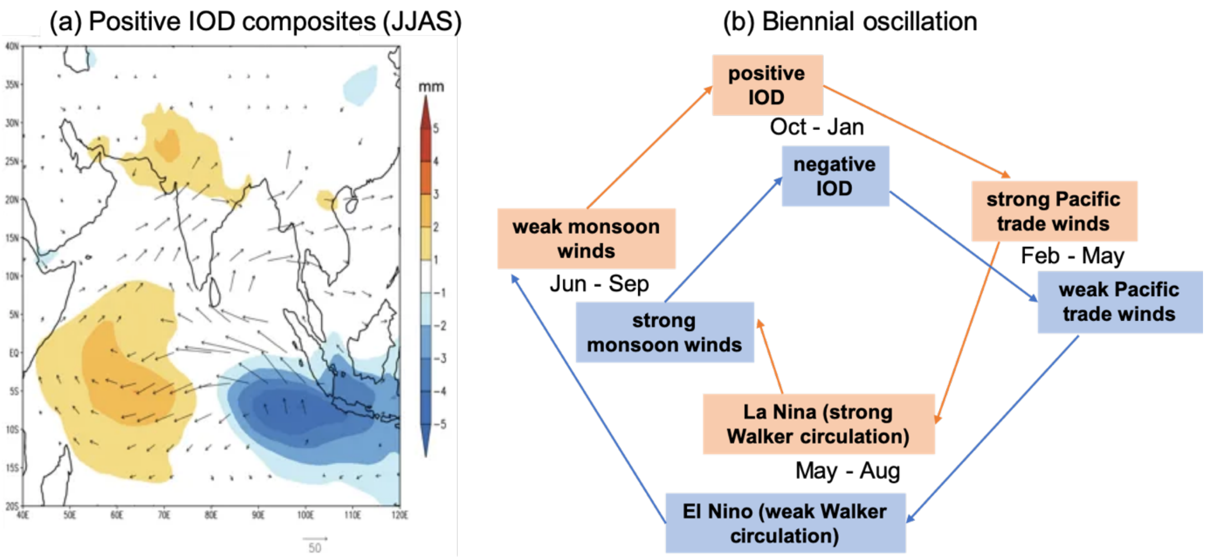

Fig. 8-3: (a) Positive IOD composite of specific humidity (mm, shaded) and moisture flux (integrated up to 300 hPa, kg/m/s, vectors) anomalies averaged in summer (JJAS). The figure is taken from Behera

and Ratnam (2018); (b) schematic of the IOD influence on ISM rainfall embedded in the TBO (adapted from the scheme in Webster and Hoyos (2010)).

In the absence of ENSO, IOD still exists (usually known as “pure IOD”) and its variability is mainly driven by the eastern Indian Ocean in a suite of coupled climate model simulations nudging the tropical Pacific SSTs toward an SST climatology estimated from observations or a control simulation (Cretat et al., 2017, 2018), as consistently seen in other coupled model studies (Gualdi et al., 2003; Fischer et al., 2005; Behera et al., 2005, 2006; Luo et al., 2010; Izumo et al., 2010; Wang et al., 2016, 2019). In the nudged experiments, the strong diabatic heating associated with enhanced rainfall over the eastern IOD lobe modulates the local Hadley circulation and induces a negative (positive) rainfall anomaly in the northern Indian Ocean during boreal summer during negative (positive) IOD events, as suggested from observational studies (Fig. 8-4; Cretat et al., 2017). Such changes in the local Hadley circulation are attenuated in the presence of ENSO because ENSO-induced changes in the (zonal) Walker circulation dominate (Cretat et al., 2017). It has also been found that rainfall anomalies over India associated with these pure IODs are modest and not statistically significant, especially at the beginning of the monsoon, although the simulated SST variability in the eastern Indian Ocean is overestimated (Fischer et al., 2005; Terray et al., 2012; Cretat et al., 2017, 2018). However, pure IODs promote a quadrupole rainfall pattern linking the tropical Indian Ocean and the Western North Pacific, and induce important zonal shifts of the Walker circulation in the absence of ENSO (Fig. 8-4), in agreement with earlier findings (Li et al., 2006; Chowdary et al., 2011). The circulation patterns with and without ENSO largely differ, confirming potential opposite effects between IOD and ENSO (e.g., Ashok et al., 2001; Lau and Nath, 2012; Pepler et al., 2014).

Pure IOD events may also help sustaining the TBO: a stronger-than-observed biennial spectrum of the IOD is found after removing ENSO's impacts (Behera et al., 2006; Cretat et al., 2018). Moreover, coupled ocean-atmosphere interactions in the Indian Ocean can sustain its own TBO without ENSO (Cretat et al., 2018). First, subsurface ocean dynamics play a key role in the biennial anomalies during boreal winter (Rao et al., 2002, 2009; Schott et al., 2009; McPhaden and Nagura, 2014; Delman et al., 2016) with a sudden reversal of thermocline anomalies in the eastern equatorial Indian Ocean forced by intra-seasonal disturbances reminiscent of the Madden-Julian Oscillation (MJO; Rao and Yamagata, 2004; Han et al., 2006). Second, tropical-extra-tropical interactions within the Indian Ocean appear to be the main trigger of IODs in the absence of ENSO (Cretat et al., 2018). In nudged experiments, both the power spectra of the ISMR and IOD indices during boreal summer shift toward increased biennial variability compared to the control simulation, which may be more consistent with a possible coupling of the IOD with ISM in the absence of ENSO, but in a regional TBO framework (Cretat et al., 2018). However, this TBO framework is again mainly based on the strong influence of the ISM circulation on the Indian Ocean SSTs despite the absence of ENSO in the nudged experiments.

In synthesis, these recent modeling studies do suggest that IOD exists without ENSO, but the exact relationships between IOD and ISM remain elusive, even in the absence of ENSO.

8.4 Past, present and future IOD influence on the ENSO-monsoon teleconnection

At long time scales, the influence of IOD on ISM seems opposite to the effect of ENSO, and the IOD-ISM rainfall relationship seems to vary complementarily to that between ENSO and ISM (Ashok et al., 2001; Krishnaswamy et al., 2015). In fact, the IOD–ISM relationship has strengthened in the recent decades (Ashok et al., 2001, 2004; Ashok and Saji, 2007; Izumo et al., 2010; Ummenhofer et al., 2011) due to non-uniform warming of the Indian Ocean (Ihara et al., 2007; Cai et al., 2009), while the ENSO–ISM relationship has weakened (Kumar et al., 1999; Ashrit et al., 2001; Ihara et al., 2007).

On longer IOD records, changes in frequency and teleconnections have been identified (e.g. Abram et al., 2008; Kayanne et al., 2006; Abram et al., 2020). Coral proxy records from Lake Victoria in Kenya suggest that the influence of ENSO has decreased over the western Indian Ocean in recent decades (Nakamura et al., 2009). A mode shifts in IOD variability related to the warming trend in the western Indian Ocean has raised the mean SST to a threshold value that encourages tropical convections (Nakamura et al., 2009). A recent reconstruction of the last millennium indicates clustering of positive IOD events with extreme IOD variability and a persistent tropical Indo-Pacific climate coupling (Abram et al., 2020). The frequency and strength of IOD events exceptionally increased during the twentieth century associated with enhanced upwelling in the eastern pole of the IOD, likely making more direct the influence of the IOD on the Asian monsoon (Abram et al., 2008). These processes and associated changes in the Walker circulation, linked to global warming, may precondition the mean state to trigger frequent positive IOD events, together with intense short rains in East Africa.

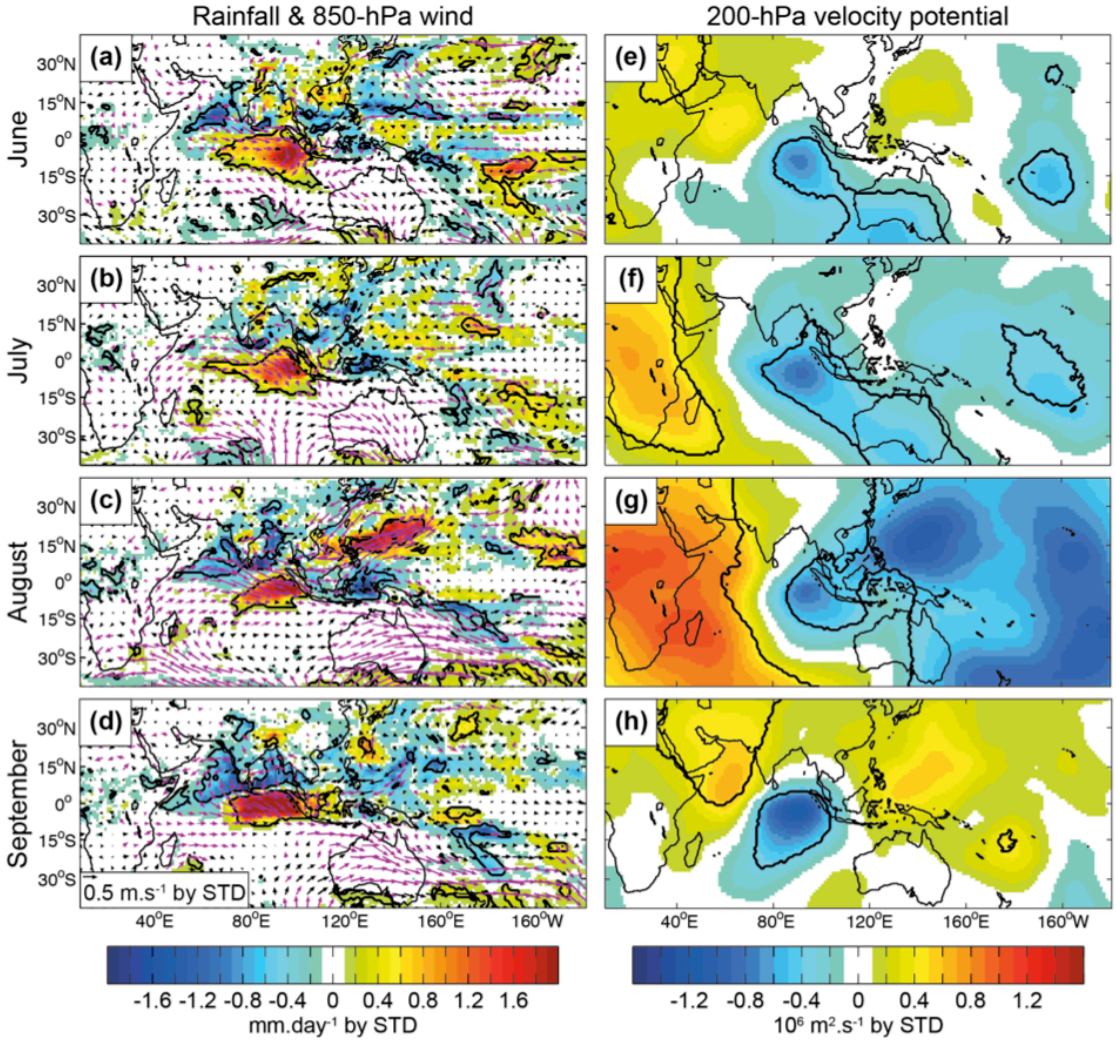

Fig. 8-4: June to September (a-d) rainfall (shading), 850-hPa wind (vectors), and (e-h) 200-hPa velocity potential anomalies regressed onto normalized boreal fall (i.e., SON) SST anomalies over the eastern IOD pole (90°E–110°E, 10°S–0°) when ENSO is removed. Significant anomalies at the 90% level are shown with black contours for rainfall and 200-hPa velocity potential anomalies, and with purple vectors for 850-hPa wind anomalies. Positive 200-hPa velocity potential anomalies correspond to abnormal upper-level mass flux convergence. Adapted from Cretat et al. (2017).

In the 20th century, the ENSO-IOD correlation was strongly positive and significant since mid-60s (Cherchi and Navarra, 2013), with ENSO and IOD almost independent before 1970 (Yuan and Li, 2008). A recent weakening of the coupling has been identified during

1999-2014 compared to the previous two decades (i.e., 1979-1998), associated with different spatial patterns in ENSO evolution during boreal spring and summer (Ham et al., 2017). The stronger/weaker correlation may correspond with either strong or weak ENSO-monsoon relationship and with strong or weak IOD-monsoon relationship, with differences arising from the relationship between Indian monsoon rainfall and SST in other ocean basins rather than the Indo-Pacific sector alone (Cherchi and Navarra, 2013).

The IOD-ENSO-ISMR relationship appears to work differently with different seasons (Agrawal et al 2017). The connection between ISM and IOD is mostly confined in the summer and autumn, while that with ENSO is stronger and extends more in time (Cherchi and Navarra, 2013). In fact, the evolution of the correlation between ISMR and monthly NINO3.4 is maximum in August-November, remaining strong and stable until March of the following year (Gershunov et al., 2001).

The 1997 El Niño was one of the strongest events occurred in the 20th century, but ISMR was slightly above normal (Srinivasan and Nanjundiah, 2002), and this has been attributed to the influence from the Indian Ocean (Slingo and Annamalai, 2000; Sreejith et al., 2015). Similarly, the influence of IOD helped nullify the effect of ENSO on the monsoon during 1997 (Saji et al., 1999; Webster et al., 1999). Positive IOD events, as those occurred during 2007-2008, co-existed with La Niña episodes (e.g. Ashok et al., 2003; Cai et al., 2009). A very strong positive IOD event occurred in the summer of 1994, as a clear coupled ocean-atmosphere phenomenon of the Indian Ocean (Behera et al., 1999). The 1994 event lasted more than 8 months from March to October and positively influenced the ISMR that recorded 265 mm/month, a value 19% above the climatological mean (Guan and Yamagata, 2003).

In 2019 the monsoon onset was delayed by about 7 days over India with the June rainfall recording a deficit of about 33% with respect to the climatological mean (Gadgil et al., 2019; http://www.imd.gov.in). According to the India Meteorology Department (IMD), subsequent to this monsoon onset, the further northward progression of the monsoon remained slow due to the formation of a very severe cyclone over central eastern Arabian Sea (i.e., the cyclone VAYU that formed during 10-17th June 2019, https://mausam.imd.gov.in/imd_latest/contents/season_report.php). El Niño weakened in July while a strong positive IOD started to develop (Fig. 8-5b) and rainfall picked up strength during the latter stages of the monsoon season (late July to September; Fig. 8-5b-d), remaining above normal. For that year, the seasonal rainfall recorded for India has been quantified at 110% of the long period average as defined by IMD, with the September rainfall beeing 152%. The positive IOD that occurred during late summer in 2019 was one of the strongest in the recent times (Fig. 8-2), with its predictability linked with the existence of the El Niño Modoki in the Equatorial Pacific (Doi et al., 2020) and to a strong pressure dipole between the Australian High and the South China Sea/Philippine Sea region (Lu and Ren, 2020). The exceptional intensity of the event remains even after the IOD index is detrended (not shown). This very recent case illustrates how the interactions between ISM, IOD, and ENSO are subtle and complex, and highly influenced by internal dynamical processes.

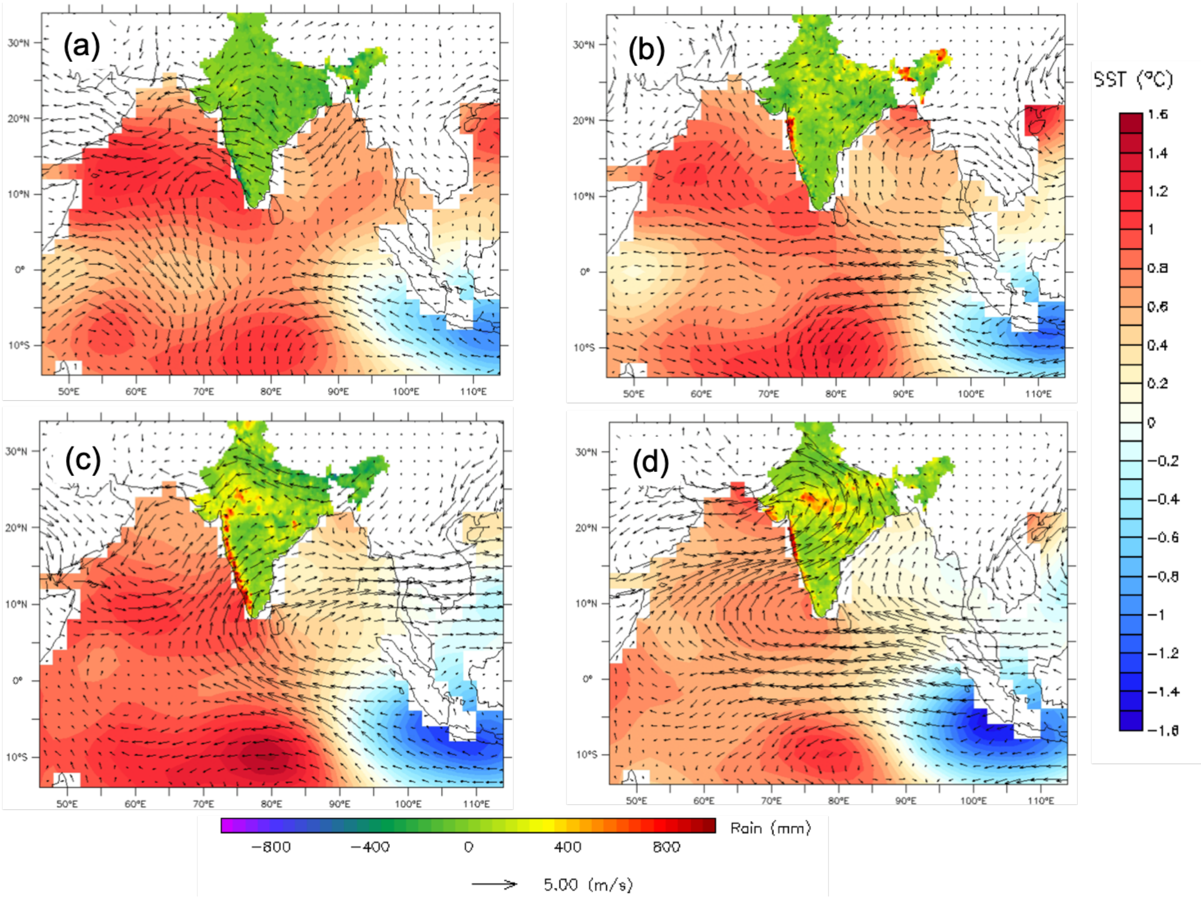

Fig. 8-5: 2019 case from (a) June to (d) September for SST (°C), 850 hPa winds (m/s), and precipitation (mm) anomalies with respect to 1980-2010 mean climatology. SST data is taken from ERSSTv5 (Huang et al. 2017), 850 hPa wind vectors are obtained from ECMWF ERA5 reanalysis (Hersbach and Dee, 2016) and precipitation from daily gridded rainfall dataset over India (Pai et al. 2014).

In the Coupled Model Intercomparison Project Phase 5 (CMIP5) models a correct representation of the coupled processes (i.e., Bjerknes feedback) in the equatorial Indian Ocean is a necessary condition for realistic monsoon simulations (Annamalai et al., 2017). At the same time, a too weak rainfall over the Arabian Sea in model may generate a warm SST bias over the western equatorial Indian Ocean that in the following fall may amplify the error toward an IOD-like SST bias via the Bjerknes feedback (Li et al., 2015). The unrealistic present-day IOD-ISMR correlation simulated by the majority of CMIP5 models may also be related to an overly strong control by ENSO (Li et al., 2017), likely leading to an underestimation of the projected future ISMR increase. Still, CMIP5 models project an increase in ISMR in a warmer climate with a reasonably strong consensus among models (Jayashankar et al., 2015). CMIP5 models' projections tend to exhibit a positive IOD-like pattern in the tropical Indian Ocean with weaker (stronger) warming in the east (west) and an easterly wind trend (Zheng et al., 2010; 2013). The response is driven by the projected weakening of the Walker circulation in a warmer climate in the majority of models (Vecchi et al., 2006; Kociuba and Power, 2015).

In future projections, surface moisture increase dominates the changes in rainfall associated with the IOD, while IOD related SST changes dominate the corresponding changes in the circulation, decreasing at a rate of 13.7%/°C (Huang et al., 2019). The ensemble spread in the IOD amplitude change is large (Ng et al., 2018), and it is related to that of the ENSO amplitude change (Hui and Zheng, 2018). The large spread in the IOD response to increasing Greenhouse Gases (GHGs) with significant variations in the amplitude and skewness of the dipole and in climatological zonal SST gradient is due to small differences in the mean thermocline depth induced by internal climate variability via the positive Bjerknes feedback (Ng et al 2018).

The frequency of extreme IOD events is projected to increase under global warming conditions (Cai et al., 2014, also see Chapter-21), with a persistence of the ENSO-IOD linkage in a warmer future world (Stuecker et al., 2017). The characteristics of the ENSO-IOD are likely to continue in the future, and given that ENSO and its predictability are modulated on decadal timescales (i.e., Wittenberg, 2009; Wittenberg et al., 2014;

Karamperidou et al., 2014), the same should be expected for the IOD (Stuecker et al., 2017).

CMIP6 models largely improved in the simulation of the spatial and temporal pattern of the ISM (Gusain et al., 2020), especially over the Western Ghats and the foothills over the Himalayas, whereas a majority of the CMIP5 models underestimated rainfall over central and northern India (Jain et al., 2019). A subset of CMIP6 models (Table 1) confirms CMIP5 results, with a tendency toward larger IOD amplitude at the end of the 20th century and in the future, at least under the most extreme CMIP6 scenario SSP5-8.5 (Fig. 8-6a). SSP stands for Shared Socioeconomic Pathways with 5 representing an economic vision of the future with relatively optimistic trends for human development but assuming an energy-intensive, fossil-fuel economy, and 8.5 corresponding to the forcing (in W/m^2) by 2100 (O'Neill et al., 2016). In summer (JJAS mean), SST regressed onto the IOD index project larger IOD-related anomalies over the Pacific and Indian Oceans (Fig. 8-6b,c). In the projection, precipitation and winds regressed onto the IOD index show modest positive anomalies over India and weaker easterlies along the Equator because of a weaker negative pole (Fig. 8-6d,e). This figure is just a flavor of the complex relationship as projected in the new generation of coupled climate models. For example, the methodology applied does not fully disentangle how the mean state changes and its role. A more systematic analysis and comparison of CMIP5 and CMIP6 experiments would be needed to fully understand differences and potential improvements. This is outside the scope of this chapter but it is under investigation in separated ongoing researches.

Table 8.1: List and some characteristics of CMIP6 models used. More details about the models can be found at https://pcmdi.llnl.gov/CMIP6/

Model Name	Institute/Country	Atmosphere	Ocean Resolution	Earth System

		Resolution (km)	(km)	Model
ACCESS-CM2	CSIRO-ARCCSS/Australia	250	100	no
ACCESS-ESM1-5	CSIRO-ARCCSS/Australia	250	100	yes
BCC-CSM2-MR	BCC/China	100	50	no
CESM2	NCAR/US	100	100	yes
CESM2-WACCM	NCAR/US	100	100	yes
CNRM-CM6-1	CNRM-CERFACS/France	250	100	no
CNRM-CM6-1-HR	CNRM-CERFACS/France	100	25	no
CNRM-ESM2-1	CNRM-CERFACS/France	250	100	yes
CanESM5	CCCma/Canada	500	100	yes
EC-Earth3	EC-Earth-Consortium/Europe	100	100	no
EC-Earth3-Veg	EC-Earth-Consortium/Europe	100	100	no
FGOALS-f3-L	CAS/China	100	100	no
FGOALS-g3	CAS/China	250	100	no
GFDL-ESM4	NOAA-GFDL/US	100	50	yes
HadGEM3-GC31-LL	MOHC-NERC/UK	250	100	no
INM-CM4-8	INM/Russia	100	100	no
INM-CM5-0	INM/Russia	100	50	no
IPSL-CM6A-LR	IPSL/France	250	100	yes
KACE-1-0-G	NIMS-KMA/South Korea	250	100	no
MCM-UA-1-0	UA/US	250	250	no
MIROC-ES2L	MIROC/Japan	500	100	yes
MIROC6	MIROC/Japan	250	100	no
MPI-ESM1-2-HR	MPI-M DWD DKRZ/Germany	100	50	yes
MPI-ESM1-2-LR	MPI-M AWI/Germany	250	250	yes
MRI-ESM2-0	MRI/Japan	100	100	yes
NESM3	NUIST/China	250	100	no
NorESM2-LM	NCC/Norway	250	100	yes
NorESM2-MM	NCC/Norway	100	100	yes
UKESM1-0-LL	MOHC NERC NIMS-KMA NIWA/UK	250	100	yes

8.5 Challenges and future perspectives

The main challenges in having a complete picture of the influence of IOD on the ENSO-ISM teleconnection remains related to a full understanding of the IOD itself and to a full and agreed understanding of how the IOD is related to ENSO on one side, and its pure (i.e., independent from ENSO) relationship with ISM on the other. While some progress have been made in recent decades in simulating ENSO variability (Bellenger et al., 2014), many important issues remain open due to the unavailability of long term observational record and the biases in state-of-the-art climate models affecting ISM and the Indian Ocean simulations(Li et al., 2015; Annamalai et al., 2017).

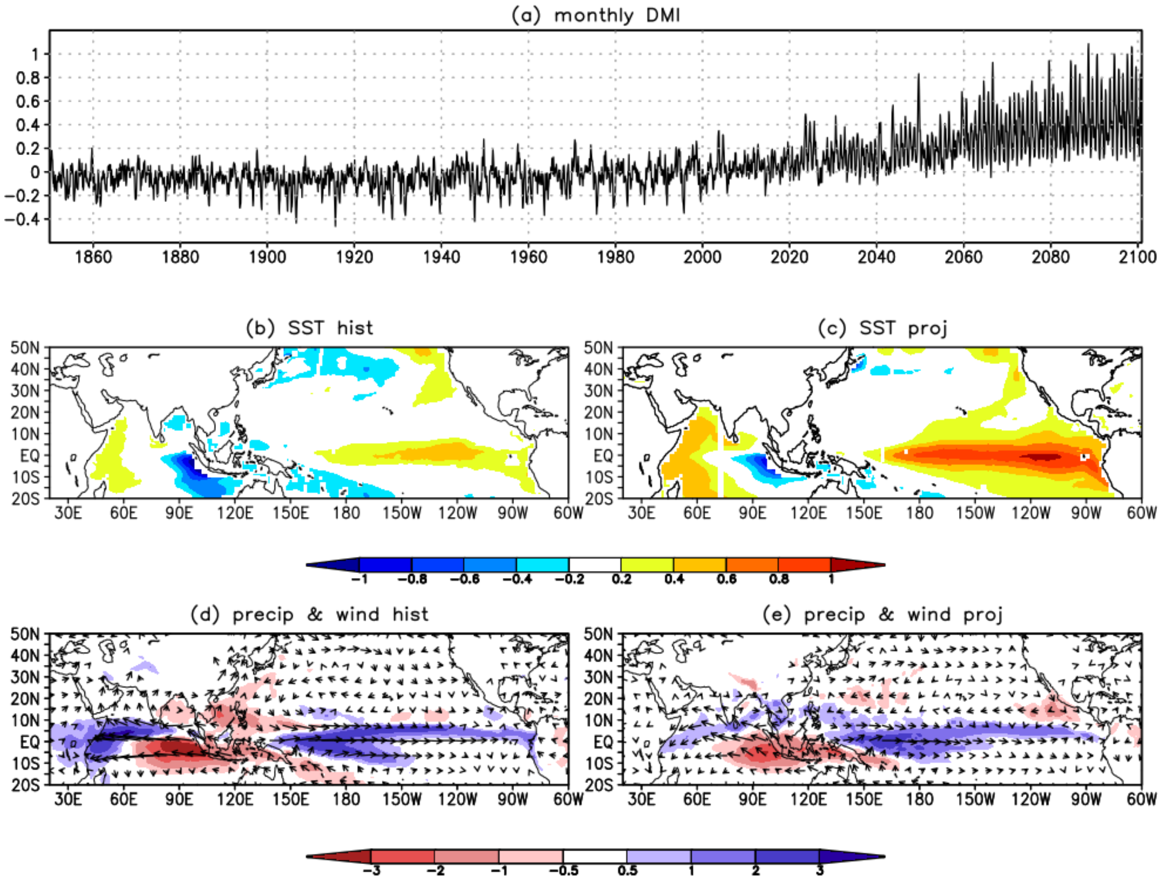

Fig. 8-6: (a) Monthly DMI index (anomalies, °C) for 20th and 21st centuries from a subset of CMIP6 models (Table 8.1). The index has been computed as in Fig. 8-2 (same areas difference and anomalies with respect to the 1980-2010 mean climatology). The index has been computed for each model and then averaged to obtain the ensemble mean. (b,c) SST (°C, shaded) and (d,e) precipitation (mm/day, shaded) and 850 hPa wind (m/s, vectors) regressed on the DMI index (values for 1°C change in the index) for JJAS mean during the historical period and the future projection, respectively. One member for each model has been considered. For the 21st century, the SSP5-8.5 scenario has been used. In panels c and e, the time-series have been detrended before computing the regression, to keep out the trend from the related variability.

An exhaustive analysis of the IOD recorded past events would allow a categorization of the main characteristics of the processes at play, but the observed record remains short to have a statistically robust assessment. On the other hand, in state-of-the-art coupled climate models the simulation of the IOD, ISM, and related characteristics (including mean state and variability) still has large biases thus precluding a complete understanding of the processes at work. For example, it is not clear whether the weak IOD-monsoon relationship simulated in the models (Fig. 8-6) is realistic or not, due to the exaggerated IOD variability or to the overly strong control of ENSO simulated by current global climate models. Moreover, it has to be clarified whether poor simulations of other factors, like IOD-induced cross-equatorial flows, may be important. Similarly, a complete understanding of the coupling and feedback processes between the developing phase of the IOD and the ISMR, including the possible feedback on the development of the IOD in the subsequent season, is still missing. As a consequence, much more in-depth observational and modeling studies (including model's improvements) are clearly needed to understand the IOD effect on ISM and the relative roles of remote versus local forcing on the ISM-ENSO relationship as well as the role of internal atmospheric processes in modulating that relationship. In future climate projections, it would be useful to understand how changes in the simulated IOD properties contribute to the relative importance of thermodynamic and dynamic monsoon processes at play in global warming frameworks.

For all the points above, crucial keys are the collection of as much as possible observations during known IOD events, and how IOD and related properties are simulated in state-of-the-art climate models. The need for more observations in the Indian Ocean is particularly important because of its changes within the last warm decades (Hermes et al., 2019). For the simulation of IOD and related models' performance, more efforts should be dedicated to reducing systematic biases in coupled climate models and/or in performing ad-hoc sensitivity experiments in a large set of different coupled models to clarify the dynamics involved in IOD formation and related teleconnections. One possibility is to design coordinated international efforts with specific common experiments, likely following current CMIP frameworks (Zhou et al., 2016) or the CORE-II experiments (Rahaman et al., 2020).

8.6 Conclusions

The IOD is one of the dominant modes of SST variability of the tropical Indian Ocean. It is recognized as having important teleconnections worldwide but here it has been considered in terms of its influence on the ISM and its relationship with ENSO. In particular, the literature focused on its active or passive role has been reviewed, evidencing how the influence of the IOD on the ISM rainfall can be interpreted as having a direct impact through moisture transport over the western Indian Ocean or modifications of the local Hadley cell, or alternatively in the framework of the tropospheric biennial oscillation. Recently, more literature is available on the role of the IOD independently from ENSO, or even as a trigger of ENSO itself. Still, combining modelling and observational studies, the precise relationship between IOD and ISM remains elusive, with or without ENSO.

Considering major ENSO and/or IOD events, it has been recorded how in 1997 the failure of the negative relationship between ENSO and the ISM rainfall was associated with a positive IOD event developing that summer, or how the strong IOD of 1994 has been responsible for a stronger than normal monsoon that summer. Recently, the strongest IOD event recorded in 2019 and its evolution within the summer evidenced how the interactions between ISM, IOD, and ENSO are complex, and highly influenced by internal dynamical processes.

CMIP5 and CMIP6 models agree in projecting stronger IOD events in the future (also see Chapter 21), but how this project on atmospheric anomalies over the Indo-Pacific region may not be fully consistent. A systematic analysis of the two model intercomparisons sets is needed to fully understand the possible differences.

Conflict of interest statement: On behalf of all authors, the corresponding author states that there is no conflict of interest.

Acknowledgments:

CINECA is acknowledged for providing resources for the storage of CMIP6 data via the "CMIP6_EC" DRES space. All CMIP6 simulations used are also freely available from the Earth System Grid Federation (https://esgf-node.llnl.gov/search/cmip6/). SBR is supported by the Belmont Forum and JPI-Climate project INTEGRATE (An Integrated data-model study of interactions between tropical monsoons and extratropical climate variability and extremes) with funding by UK NERC grant NE/P006809/1. SS gratefully acknowledges the financial support given by the Ministry of Earth Sciences, Government of India to support the ST Radar facility at ACARR, CUSAT, Kochi. The Centre for Climate Change Research (CCCR) at Indian Institute of Tropical Meteorology (IITM) is fully funded by the Ministry of Earth Sciences, Government of India. PT is funded by Institut de Recherche pour le Développement (IRD, France).

References

Abram, N.J., Wright, N.M., Ellis, B., Dixon, B.C., Wurtzel, J.B., England, M.H., Ummenhofer, C.C., Philibosian, B., Chayarini, S.Y., Yu, T.-L., Shen, C.-C., Cheng, H., Edwards, L., Heslop, D., 2020. Coupling of Indo-Pacific climate variability over the last millennium. Nature, 579, 385-392 doi: 10.1038/s41586-020-2084-4

Abram, N.J., Gagan, M.K., Cole, J.E., Hantoro, W.S., Mudelsee, M., 2008. Recent intensification of tropical climate variability in the Indian Ocean. Nat. Geosci. 1, 849–853 doi: 10.1038/ngeo357

Agrawal, N., Pandey, V.K., Shahi, N., 2017. ENSO-IOD changing relationship and its impact on Indian Summer Monsoon. VSRD Intern. J. Tech. Non-Tech. Res. 8(5), 165-74

Allan, R., Chambers, D., Drosdowsky, W., Hendon, H., Latif, M., Nicholls, N., Smith, I., Stone, R., Tourre, Y., 2001. Is there an Indian Ocean dipole and is it independent of the El Niño-Southern Oscillation? CLIVAR Exch. 6, 18–22

Anil, N., Ramesh Kumar, M.R., Sajeev, R., Saji, P. K., 2016. Role of distinct flavors of IOD events on Indian summer monsoon. Natural Hazards 82, 1317-1326 doi: 10.1007/s11069-016-2245-9

Annamalai, H., Taguchi, B., McCreary, J.P., Nagura, M., Miyama, T., 2017. Systematic errors in South Asian monsoon simulation: Importance of equatorial Indian Ocean processes. J. Clim. 30, 8159-8178 doi: 10.1175/JCLI-D-16-0573.1

Annamalai, H., Liu, P., Xie, S.P., 2005. Southwest Indian Ocean SST variability: its local effect and remote influence on Asian monsoons. J. Clim. 18(20), 4150-4167 doi: 10.1175/JCLI3533.1

Annamalai, H., Murtugudde, R., Potemra, J., Xie, S.P., Liu, P., Wang, B., 2003. Coupled dynamics over the Indian Ocean: Spring initiation of the zonal mode. Deep-Sea Res. II 50, 2305-2330 doi: 10.1016/S0967-0645(03)00058-4

Ashok, K., Guan, Z., Yamagata, T., 2003. A look at the relationship between the ENSO and the Indian Ocean dipole. J. Meteor. Soc. Japan 81, 41-56 doi: 10.2151/jmsj.81.41

Ashok, K., Guan, Z., Saji, N.H., Yamagata, T., 2004. Individual and combined influences of ENSO and the Indian Ocean dipole on the Indian summer monsoon. J. Clim. 17, 3141-3155 doi: 10.1175/1520-0442(2004)017<3141:IACIOE>2.0.CO;2

Ashok, K., Guan, Z., Yamagata, T., 2001. Impact of Indian Ocean dipole on the relationship between the Indian monsoon rainfall and ENSO. Geophys. Res. Lett. 28, 4499-4502 doi: 10.1029/2001GL013294

Ashok, K., Saji, N.H., 2007. On impacts of ENSO and Indian Ocean dipole events on the sub-regional Indian summer monsoon rainfall. Nat. Haz. 42(2), 273-285 doi: 10.1007/s11069-006-9091-0

Ashrit, R.G., Kumar, K.R., Kumar, K.K., 2001. ENSO-Monsoon relationships in a greenhouse warming scenario. Geophys. Res. Lett. 28, 1727- 1730 doi: 10.1029/2000GL012489

Baquero-Bernal, A., Latif, M., Legutke, S., 2002. On dipole-like variability of sea surface temperature in the Indian Ocean. J. Clim. 15, 1358-1368 doi: 10.1175/1520-0442(2002)015<1358:ODVOSS>2.0.CO;2

Bazo, J., de las Nieves Lorenzo, M., Porfirio da Rocha, R., 2013. Relationship between monthly rainfall in NW Peru and tropical sea surface temperature. Adv. Meteor. doi: 10.1155/2013/152875

Behera, S.K., Krishnan, R., Yamagata, T., 1999. Unusual ocean–atmosphere conditions in the tropical Indian Ocean during 1994. Geophys. Res. Lett. 26, 3001-3004 doi: 10.1029/1999GL010434

Behera, S.K., Rao, S.A., Saji, N.H., Yamagata, T., 2003. Comments on “A cautionary note on the interpretation of EOFs¨. J. Clim. 16, 1094-1097 doi: 10.1175/1520-0442(2003)016<1087:COACNO>2.0.CO;2

Behera, S.K., Luo, J.J., Masson, S., Delecluse, P., Gualdi, S., Navarra, A., Yamagata, T., 2005. Paramount impact of the Indian Ocean dipole on the East African short rains: a CGCM study. J. Clim. 18, 4514-4530 doi: 10.1175/JCLI3541.1

Behera, S.K, Luo, J.J., Masson, S., Rao, S.A., Sakuma, H., Yamagata, T., 2006. A CGCM study on the interaction between IOD and ENSO. J. Clim 19, 1608-1705 doi: 10.1175/JCLI3797.1

Behera, S. K., Ratnam, J.V., Masumoto, Y., Yamagata, T., 2012. Origin of extreme summers in Europe - The Indo-Pacific connection. Clim. Dyn. doi: 10.1007/s00382-012-1524-8

Behera, S.K., Yamagata, T., 2003. Influence of the Indian Ocean dipole on the Southern Oscillation. J. Meteor. Soc. Jpn 81(1), 169-177 doi: 10.2151/jmsj.81.169

Behera, S.K., Ratnam, J.V., 2018. Quasi-asymmetric response of the Indian summer monsoon rainfall to opposite phases of the IOD. Sci. Rep. doi:10.1038/s41598-017-18396-6

Bellenger, H., Guilyardi, E., Leloup, J., Lengaigne, M., Vialard, J., 2014. ENSO representation in climate models: from CMIP3 to CMIP5. Clim. Dyn. 42, 1999-2018 doi: 10.1007/s00382-013-1783-z

Black, E., Slingo, J., Sperber, K.R., 2003. An observational study of the relationship between excessively strong short rains in coastal East Africa and Indian Ocean SST. Mon. Wea. Rev. 31, 74-94 doi: 1175/1520-0493(2003)131<0074:AOSOTR>2.0.CO;2

Boschat, G., Terray, P., Masson, S., 2011. Interannual relationships between Indian summer monsoon and Indo-Pacific coupled modes of variability during recent decades. Clim. Dyn. 37, 1019-1043 doi: 10.1007/s00382-010-0887-y

Boschat, G., Terray, P., Masson, S., 2012. Robustness of SST teleconnections and precursory patterns associated with the Indian summer monsoon. Clim. Dyn. 38, 2143-2165 doi: 10.1007/s00382-011-1100-7

Cai, W., Wu, L., Lengaigne, M., Li, T., McGregor, S., Kug, J.-S., Yu, J.-Y., Stuecker, M.F., Santoso, A., Li, X., Ham, Y.-G., Chikamoto, Y., Ng, B., McPhaden, M.J., Du, Y., Dommenget, D., Jia, F., Kajtar, J.B., Keenlyside, N., Lin, X., Luo, J.J., Martin-Rey, M., Ruprich-Robert, Y., Wang, G, Xie, S.P., Yang, Y., Kang, S.M., Choi, J.-Y., Gan, B., Kim, G.-I., Kim, C.-E., Kim, S., Kim, J.-H., Chang, P., 2019. Pantropical climate interactions. Science 363, 6430 doi: 10.1126/science.aav4236

Cai, W., Santoso, A., Wang, G., Weller, E., Wu, L., Ashok, K., Masumoto, Y. and Yamagata, T., 2014. Increased frequency of extreme Indian Ocean Dipole events due to greenhouse warming. Nature 510(7504), 254-258 doi: 10.1038/nature13327

Cai, W., Sullivan, A., Cowan, T., 2011. Interactions of ENSO, the IOD, and the SAM in CMIP3 models. J. Clim. 24(6), 1688-1704 doi: 10.1175/2010JCLI3744.1

Cai, W., Sullivan, A., Cowan, T., 2009. Climate change contributes to more frequent consecutive positive Indian Ocean dipole events. Geophys. Res. Lett. 36, L23704 doi:10.1029/2009GL040163

Chan, S., Behera, S., Yamagata, T., 2008. The Indian Ocean Dipole teleconnection to South America. Geophys. Res. Lett. 35, L14S12 doi:10.1029/2008GL034204

Chen, W., Wang, L., Feng, J., Wen, Z., Ma, T., Yang, X., Wang, C., 2019. Recent progress in studies of the variabilities and mechanisms of the East Asian monsoon in a changing climate. Adv. Atm. Sci. 36, 887-901 doi: 10.1007/s00376-019-8230-y

Cherchi, A., Navarra, A., 2013. Influence of ENSO and of the Indian Ocean Dipole on the Indian summer monsoon variability. Clim. Dyn. 41, 81-103 doi: 10.1007/s00382-012-1602-y

Cherchi, A., Gualdi, S., Behera, S., Luo, J.J., Masson, S., Yamagata, T., Navarra, A., 2007. The influence of tropical Indian Ocean SST on the Indian summer monsoon. J. Clim. 20, 3083-3105 doi: 10.1175/JCLI4161.1

Chowdary, J. S., Gnanaseelan, C., Xie, S. P., 2009. Westward propagation of barrier layer formation in the 2006-07 Rossby wave event over the tropical southwest Indian Ocean. Geophys. Res. Lett. 36(4). doi:10.1029/2008gl036642.

Chowdary, J.S. and Gnanaseelan, C., 2007. Basin□wide warming of the Indian Ocean during El Niño and Indian Ocean dipole years. Inter. J. Clim., 27(11), 1421-1438.

Chowdary, J.S., Bandgar, A.B., Gnanaseelan, C. and Luo, J.J., 2015. Role of tropical Indian Ocean air–sea interactions in modulating Indian summer monsoon in a coupled model. Atmos. Sci. Lett., 16(2), pp.170-176.

Chowdary, J.S., Xie, S.P., Luo, J.J., Hafner, J., Behera, S., Masumoto, Y., Yamagata, T., 2011. Predictability of Northwest Pacific climate during summer and the role of the tropical Indian Ocean. Clim. Dyn. 36, 607-621 doi: 10.1007/s00382-009-0686-5

Cretat, J., Terray, P., Masson, S., Sooraj, K.P., Roxy, M.K., 2017. Indian Ocean and Indian Summer Monsoon: relationships without ENSO in ocean-atmosphere coupled simulations. Clim. Dyn. 49, 1429-1448 doi: 10.1007/s00382-016-3387-x

Cretat, J., Terray, P., Masson, S., Sooraj, K.P., 2018. Intrinsic precursors and timescale of the tropical Indian Ocean Dipole: Insights from partially decoupled experiment. Clim. Dyn. 51, 1311-1352 doi: 10.1007/s00382-017-3956-7

Delman, A.S., Sprintall, J., McClean, J.L., Talley, L.D., 2016. Anomalous Java cooling at the initiation of positive Indian Ocean Dipole events. J. Geophys. Res. Oc. doi:10.1002/2016JC011635

Dey, R., Lewis, S.C., Abram, N.J., 2019. Investigating observed northwest Australian rainfall trends in coupled model intercomparison project phase 5 detection and attribution experiments. Int. J. Climatol. 39, 112-127 doi: 10.1002/joc.5788

Doi, T., Behera, S.W., Yamagata, T., 2020, Predictability of the super IOD event in 2019 and its link with El Niño Modoki. Geophys. Res. Lett. 47, e2019GL086713 doi: 10.1029/2019GL086713

Dommenget, D., Latif, M., 2002. A cautionary note on the interpretation of EOFs. J. Clim. 15, 216-225 doi: 10.1175/1520-0442(2002)015<0216:ACNOTI>2.0.CO;2

Dommenget, D., 2011. An objective analysis of the observed spatial structure of the tropical Indian Ocean SST variability. Clim. Dyn. 36, 2129-2145 doi: 10.1007/s00382-010-0787-1

Drbohlav, H.K.L., Gualdi, S., Navarra, A., 2007. A diagnostic study of the Indian Ocean dipole mode in El Niño and non-El Niño years. J. Clim. 20, 2961-2977 doi: 10.1175/JCLI4153.1

Du, Y., Cai, W., Wu, Y., 2013. A new type of the Indian Ocean Dipole since the mid-1970s. J. Clim. 26(3), 959-972 doi: 10.1175/JCLI-D-12-00047.1

Du, Y., Xie, S.P., Huang, G., Hu, K., 2009. Role of air-sea interaction in the long persistence of El Niño-induced North Indian Ocean warming. J. Clim. 22(8), 2023-2038 doi: 10.1175/2008JCLI2590.1

Endris, H.S., Lennard, C., Hewitson, B., Dosio, A., Nikulin G., Artan, G.A., 2019. Future changes in rainfall associated with ENSO, IOD and changes in the mean state over eastern Africa. Clim. Dyn. 52, 2029-2053 doi: 10.1007/s00382-018-4239-7

Fischer, A.S., Terray, P., Delecluse, P., Gualdi, S., Guilyardi, E., 2005. Two independent triggers for the Indian Ocean dipole/zonal mode in a coupled GCM. J. Clim. 18, 3428-3449 doi: 10.1175/JCLI3478.1

Gadgil, S., Francis, P.A., Vinayachandran, P.N., 2019. Summer monsoon of 2019: understanding the performance so far and speculating about the rest of the season. Curr. Sci. 117(5), 783-793

Gadgil, S., Vinayachandran, P.N., Francis, P.A., Gadgil, S., 2004. Extremes of the Indian summer monsoon rainfall, ENSO and equatorial Indian Ocean oscillation. Geophys. Res. Lett. 31, L12213 doi:10.1029/2004GL019733

Gadgil, S., Rajeevan, M., Nanjundiah, R., 2005. Monsoon prediction – why yet another failure? Curr. Sci. 84, 1713-1719

Gadgil, S., Rajeevan, M., Francis, P.A., 2007. Monsoon variability: links to major oscillations over the equatorial Pacific and Indian oceans. Curr. Sci. 93, 182-194

Gershunov, A., Schneider, N., Barnett, T., 2001. Low-frequency modulation of the ENSO-Indian monsoon rainfall relationship: signal or noise? J. Clim. 14, 2486-2492 doi: 10.1175/1520-0442(2001)014<2486:LFMOTE>2.0.CO;2

Goswami, B.N., 1998. Interannual variations of Indian summer monsoon in a GCM: external conditions versus internal feedbacks. J. Clim. 11, 501-521 doi: 10.1175/1520-0442(1998)011<0501:IVOISM>2.0.CO;2

Gualdi, S., Guilyardi, E., Navarra, A., Masina, S., Delecluse, P., 2003. The interannual variability in the tropical Indian Ocean as simulated by a CGCM. Clim. Dyn. 20, 567-582 doi: 10.1007/s00382-002-0295-z

Guan, Z., Ashok, K., Yamagata, T., 2003. Summer-time response of the tropical atmosphere to the Indian Ocean dipole sea surface temperature anomalies. J. Meteorol. Soc. Jpn. 81, 531-561 doi: 10.2151/jmsj.81.533

Guan, Z., Yamagata, T., 2003. The unusual summer of 1994 in East Asia: IOD teleconnections. Geophys. Res. Lett. 30 doi:1029/2002GL016831

Gusain, A., Ghosh, S., Karmakar, S., 2020. Added value of CMIP6 over CMIP5 models in simulating Indian summer monsoon rainfall. Atm. Res. 232, 104680 doi: 10.1016/j.atmosres.2019.104680

Ham, Y.-G., Choi, J.-Y., Kug, J.-S., 2017. The weakening of the ENSO-Indian Ocean Dipole (IOD) coupling strength in recent decades. Clim. Dyn. 49(1), 249-261 doi: 10.1007/s00382-016-3339-5

Han, W., Shinoda, T., Fu, L.L., McCreary, J.P., 2006. Impact of atmospheric intraseasonal oscillations on the Indian Ocean dipole during the 1990s. J. Phys. Oceanogr. 111, 679-690 doi: 10.1175/JPO2892.1

Hastenrath, S., Nicklis, A., Greischar, L., 1993. Atmospheric-hydrospheric mechanisms of climate anomalies in the western equatorial Indian Ocean. J. Geophys. Res. 98 (C11), 20219-20235 doi: 10.1029/93JC02330

Hastenrath, S., 2002. Dipoles, temperature gradients and tropical climate anomalies. Bull. Amer. Meteor. Soc. 83, 735-740 doi: 10.1175/1520-0477(2002)083<0735:WLACNM>2.3.CO;2

Hermes, J.C., Masumoto, Y., Beal, L.M., Roxy, M.K., Vialard, J., Andres, M., Annamalai, H., Behera, S., D'Adamo, N., Doi, T., Feng, M., Han, W., Hardman-Mountford, N., Hendon, H., Hood, R., Kido, S., Lee, C., Lee, T., Lengaigne, M., Li., J., Lumpkin, R., Navaneeth, K.N., Millingan, B., McPhaden, M.J., Ravichandran, M., Shinoda, T., Singh, A., Sloyan, B., Strutton, P.G., Subramanian, A.C., Thurston, S, Tozuka, T., Ummenhofer, C.C., Unnikrishnan, A.S., Venkatesan, R., Wang, D., Wiggert, J., Yu, L., Yu, W., 2019. A sustained ocean observing system in the Indian Ocean for climate related scientific knowledge and societal needs. Front. Mar. Sci. doi: 10.3389/fmars.2019.00355

Hersbach, H. and Dee, D.J.E.N., 2016. ERA5 reanalysis is in production. ECMWF Newsletter, 147(7), pp.5-6

Hong, C.C., Li, T., Ho, L., Chen, Y.C. 2010. Asymmetry of the Indian Ocean basinwide SST anomalies: Roles of ENSO and IOD. J. Clim. 23, 3563-3576 doi: 10.1175/2010JCLI3320.1

Hong, C.C., Lu, M.M., Kanamitsu, M., 2008. Temporal and spatial characteristics of positive and negative Indian Ocean dipole with and without ENSO. J. Geophys. Res. Atmos. 113, D08107 doi: 10.1029/2007JD009151

Hossain, I., Rasel, H.M., Imteaz, M.A., Mekanik, F., 2020. Long-term seasonal rainfall forecasting using linear and non-linear modelling approaches: a case study for western Australia. Meteor. Atm. Phys. 132, 131-141 doi: 10.1007/s00703-019-00679-4

Huang, B., Kinter, J.L., 2002. Interannual variability in the tropical Indian Ocean. J. Clim. 107 (C11) doi:101.1029/2001JC001278

Huang, B., Thorne, P.W., Banzon, V.F., Boyer, T., Chepurin, G., Lawrimore, J.H., Menne, M.J., Smith, T.M., Vose, R.S. and Zhang, H.M., 2017. Extended reconstructed sea surface temperature, version 5 (ERSSTv5): upgrades, validations, and intercomparisons. J. Clim. 30(20), 8179-8205

Huang, P., Zheng, X.T., Ying, J., 2019. Disentangling the changes in the Indian Ocean Dipole-related SST and rainfall variability under global warming in CMIP5 models. J. Clim. 32, 3803-3818 doi: 10.1175/JCLI-D-18-0847.1

Hui, C., Zheng, X.T., 2018. Uncertainty in Indian Ocean dipole response to global warming: the role of internal variability. Clim. Dyn. doi: 10.1007/s00382-018-4098-2

Ihara, C., Kushnir, Y., Cane, M.A., De La Peña, V.H., 2007. Indian summer monsoon rainfall and its link with ENSO and Indian Ocean climate indices. Int. J. Clim. 27, 179-187 doi: 10.1002/joc.1394

Izumo, T., de Boyer Montegut, C., Luo, J.–J., Behera, S.K., Masson S., Yamagata T., 2008. The role of the western Arabian Sea upwelling in Indian monsoon rainfall variability. J. Clim. 21, 5603-5623 doi: 10.1175/2008JCLI2158.1

Izumo, T., Vialard, J., Lengaigne, M., de Boyer Montégut, C., Behera, S.K, Luo, J.J., Cravatte, S., Masson, S., Yamagata, T., 2010. Influence of the state of the Indian Ocean Dipole on the following year's El Niño. Nature Geosci. 3, 168-172 doi: 10.1038/ngeo760

Jain, S., Salunke, P., Mishra, S.K., Sahany, S. and Choudhary, N., 2019. Advantage of NEX-GDDP over CMIP5 and CORDEX Data: Indian Summer Monsoon. Atm. Res. 228, 152-160 doi: 10.1016/j.atmosres.2019.05.026

Jayasankar, C.B., Surendran, S. and Rajendran, K., 2015. Robust signals of future projections of Indian summer monsoon rainfall by IPCC AR5 climate models: Role of seasonal cycle and interannual variability. Geophys. Res. Lett. 42(9), 3513-3520 doi: 10.1002/2015GL063659

Jourdain, N.C., Lengaigne, M., Vialard, J., Izumo, T., Sen Gupta, A., 2016. Further insights on the influence of the Indian Ocean dipole on the following year's ENSO from observations and CMIP5 models. J. Clim. 29, 637-658 doi: 10.1175/JCLI-D-15-0481.1

Kajtar, J.B., Santoso, A., England, M.H., Cai, W., 2016. Tropical climate variability: interactions across the Pacific, Indian, and Atlantic Oceans. Clim. Dyn. doi:10.1007/s00382-016-3199-z

Karamperidou, C., Cane, M.A., Lall, U., Wittemberg, A.T., 2014. Intrinsic modulation of ENSO predictability viewed through a local Lyapunov lens. Clim. Dyn. 42, 253-270 doi: 10.1007/s00382-013-1759-z

Kayanne, H., Iijima, H., Nakamura, N., McClanahan, T.R., Behera, S., Yamagata, T., 2006. The Indian Ocean Dipole Index recorded in Kenyan coral annual density bands. Geophys. Res. Lett. 33, L19709 doi:10.1029/2006GL027168

Kinter, J.L. III, Miyakoda, K., Yang, S., 2002. Recent changes in the connection from the Asian monsoon to ENSO. J. Clim. 15, 1203-1215 doi: 10.1175/1520-0442(2002)015<1203:RCITCF>2.0.CO;2

Kirtman, B., Shukla, J., 2000. Influence of the Indian summer monsoon on ENSO. Quart. J. Roy. Meteor. Soc. 126, 213-239 doi: 10.1002/qj.49712656211

Kociuba, G., Power, S.B., 2015. Inability of CMIP5 models to simulate recent strengthening of the Walker circulation: Implications for projections. J Clim 28, 20-35 doi: 10.1175/JCLI-D-13-00752.1

Krishnan, R., Mujumdar, M., Vaidya, V., Ramesh, K.V., Satyan, V., 2003. The Abnormal Indian Summer Monsoon of 2000. J. Clim. 16, 1177-1194

Krishan, R., Ayantika, D.C., Kumar, V., Pokhrel, S., 2011. The long-lived monsoon depressions of 2006 and their linkage with the Indian Ocean Dipole. Int. J. Climatol. 31, 1334-1352 doi: 10.1002/joc.2156

Krishnaswamy, J., Vaidyanathan, S., Rajagopalan, B., et al, 2015. Non-stationary and non-linear influence of ENSO and Indian Ocean Dipole on the variability of Indian monsoon rainfall and extreme rain events. Clim. Dyn. 45, 175-184 doi: 10.1007/s00382-014-2288-0

Kug, J.-S., Ham, Y.-G., 2012. Indian Ocean feedback to the ENSO transition in a multi-model ensemble. J. Clim. 25, 6942-6957 doi: 10.1175/JCLI-D-12-00078.1

Kug, J.-S., Kang, I.-S., 2006. Interactive feedback between the Indian Ocean and ENSO. J. Clim. 19, 1784-1801 doi: 10.1175/JCLI3660.1

Kumar, K.K., Rajagopalan, B., Cane, M.A., 1999. On the weakening relationship between the Indian monsoon and ENSO. Science 284, 2156-2159 doi: 10.1126/science.284.5423.2156

Lau, N.C., Nath, M.J., 2003. Atmosphere–ocean variations in the Indo-Pacific sector during ENSO episode. J. Clim. 16, 3-20 doi: 10.1175/1520-0442(2003)016<0003:AOVITI>2.0.CO;2

Lau, N.-C., Nath, M.J., 2004. Coupled GCM simulation of atmosphere-ocean variability associated with zonally asymmetric SST changes in the tropical Indian Ocean. J. Clim. 17, 245-265 doi: 10.1175/1520-0442(2004)017<0245:CGSOAV>2.0.CO;2

Lau, N.C., Nath, M.J., 2012. A Model Study of the Air–Sea Interaction Associated with the Climatological Aspects and Interannual Variability of the South Asian Summer Monsoon Development. J. Clim. 25, 839-857 doi: 10.1175/JCLI-D-11-00035.1

Lau, N.-C., Wang, B., 2006. Interactions between the Asian monsoon and the El Niño Southern Oscillation, in: Wang, B., (Eds), The Asian Monsoon. Springer-Praxis, Chichester, pp 479-511

Li, G., Xie, S.P., Du, Y., 2015. Monsoon-induced biases of climate models over the tropical Indian Ocean. J. Clim. 28, 3058-3072 doi: 10.1175/JCLI-D-14-00740.1

Li, Z., Lin, X. and Cai, W., 2017. Realism of modelled Indian summer monsoon correlation with the tropical Indo-Pacific affects projected monsoon changes. Sci. Rep. 7(1), 1-7 doi: 10.1038/s41598-017-05225-z

Li, T., Wang, B., Chang, C.P., Zhang, Y.S., 2003. A theory for the Indian Ocean dipole-zonal mode. J. Atmos. Sci. 60, 2119-2135 doi: 10.1175/1520-0469(2003)060<2119:ATFTIO>2.0.CO;2

Li, T., Liu, P., Fu, X., Wang, B., Meehl, G.A., 2006. Spatiotemporal structures and mechanisms of the Tropospheric Biennial Oscillation in the Indo-Pacific warm ocean regions. J. Clim. 19, 3070-3087 doi: 10.1175/JCLI3736.1

Loschnigg, J., Meehl, G.A., Webster, P.J., Arblaster, J.M., Compo, G.P., 2003. The Asian monsoon, the tropospheric biennial oscillation and the Indian Ocean dipole in the NCAR CSM. J. Clim. 16, 2138-2158 doi: 10.1175/1520-0442(2003)016<1617:TAMTTB>2.0.CO;2

Lu, B., Ren, H.-L., 2020. What caused the extreme Indian Ocean Dipole event in 2019? Geophys. Res. Lett. 47, e2020GL087768 doi: 10.1029/2020GL087768

Luo, J.J., Zhang, R., Behera, S.K., Masumoto, Y., Jin, F.F., Lukas, R., Yamagata, T., 2010. Interactions between El Niño and extreme Indian Ocean dipole. J. Clim. 23, 726-742 doi: 10.1175/2009JCLI3104.1

Manatsa, D., Behera, S.K., 2013. On the epochal strengthening in the relationship between rainfall of East Africa and IOD. J. Clim. 26, 5655-5673 doi: 10.1175/JCLI-D-12-00568.1

McPhaden, M.J., Nagura, N., 2014. Indian Ocean dipole interpreted in terms of recharge oscillator theory. Clim. Dyn. 42, 1569-1586 doi: 10.1007/s00382-013-1765-1

Meehl, G.A., Arblaster, J.M., 2002. Indian monsoon GCM sensitivity experiments testing tropospheric biennial oscillation transition conditions. J. Clim. 15, 923-944 doi: 10.1175/1520-0442(2002)015<0923:IMGSET>2.0.CO;2

Meehl, G.A., Arblaster, J.M., Loschnigg, J., 2003. Coupled ocean-atmosphere dynamical processes in the tropical Indian and Pacific oceans and the TBO. J. Clim. 16, 2138-2158 doi:10.1175/2767.1

Murtugudde, R., Beauchamp, J., Bussalacchi, A., Nerem, S., 1995. Secular sea-level change in the Indian Ocean: Comparison of model result with TOPEX/Poseidon data. Trans. Am. Geophys. Union (EOS), 76, G32A–63211

Murtugudde, R., Goswami, B.N., Busalacchi, A.J., 1998. Air sea interactions in the southern Indian Ocean and its relation to interannual variability of the monsoons over India. Proceedings of the International Conference on Monsoon and Hydrological Cycle, Kyongju, Korea, 184–188.

Murtugudde, R., Busalacchi, A.J., 1999. Internannual variability of the dynamics and thermodynamics of the tropical Indian Ocean. J. Clim. 12, 2300-2326 doi: 10.1175/1520-0442(1999)012<2300:IVOTDA>2.0.CO;2

Murtugudde, R., Busalacchi, A.J., McCreary, J.P., 2003. Comment on “Dipoles, temperature gradients and tropical climate anomalies”. Bull. Amer. Meteor. Soc. 84, 1422-1423 doi: 10.1175/BAMS-84-10-1422

Nakamura, N., Kayanne, H., Iijima, H., McClanahan, T.R., Behera, S.K., Yamagata, T., 2009. Mode shift in the Indian Ocean climate under global warming stress. Geophys. Res. Lett. 36, 23, L23708 doi: 10.1029/2009GL040590

Ng, B., Cai, W., Cowan, T., Bi, D., 2018. Influence of internal climate variability on Indian Ocean dipole properties. Sci. Rep. 8, 13500 doi: 10.1038/s41598-018-31842-3

O'Neill, B.C., Tebaldi, C., van Vuuren, D.P., Eyring, V., Friedlingstein, P., Hurtt, G., Knutti, R., Kriegler, E., Lamarque, J.-F., Lowe, J., Meehl, G.A., Moss, R., Riahi, K., Sanderson, B.M., 2016. The Scenario Model Intercomparison Project (ScenarioMIP) for CMIP6. Geosci. Model Dev., 9, 3461-3482 doi: 10.5194/gmd-9-3461-2016

Pai, D.S., Sridhar, L., Rajeevan, M., Sreejith, O.P., Satbhai, N.S. and Mukhopadhyay, B., 2014. Development of a new high spatial resolution (0.25× 0.25) long period (1901–2010) daily gridded rainfall data set over India and its comparison with existing data sets over the region. Mausam, 65(1), 1-18

Pepler, A., Timbal, B., Rakich, C., Coutts-Smith, A., 2014. Indian Ocean dipole overrides ENSO's influence on cool season rainfall across the eastern seaboard of Australia. J. Clim. 27, 3816-3826 doi: 10.1175/JCLI-D-13-00554.1

Rahaman, H., Srinivasu, U., Panickal, S., Durgadoo, J.V., Griffies, S.M., Ravichandran, M., Bozec, A., Cherchi, A., Voldoire, A., Sidorenko, D., Chassignet, E.P., Danabasoglu, G., Tsujino, H., Getzlaff, K., Ilicak, M., Bentsen, M., Long, M.C., Fogli, P.G., Farneti, R., Danilov, S., Marsland, S.J., Valcke, S., Yeager, S.G., Wang, Q., 2020. An assessment of the Indian Ocean mean state and seasonal cycle in a suite of interannual CORE-II simulations. Oc. Modell. doi: 10.1016/j.ocemod.2019.101503

Rao, K.G., Goswami, B.N., 1988. Interannual variations of sea surface temperature over the Arabian Sea and the Indian monsoon: a new perspective. Mon. Weath. Rev. 116, 558-568

Rao, S.A., Yamagata, T., 2004. Abrupt termination of Indian Ocean dipole events in response to intraseasonal disturbances. Geophys. Res. Lett. 31, L19306 doi:10.1029/2004GL020842

Rao, S.A., Behera, S.K., Masumoto, Y., Yamagata, T., 2002. Interannual subsurface variability in the Tropical Indian Ocean with a special emphasis on the Indian Ocean Dipole. Deep-Sea Res. 49, 1549-1572

Rao, S.A., Luo, J.J., Behera, S.K., Yamagata, T., 2009. Generation and termination of Indian Ocean dipole events in 2003, 2006 and 2007. Clim. Dyn. 33, 751-767 doi: 10.1007/s00382-008-0498-z

Rasmusson, E.M., Carpenter, T.H., 1983. The relationship between eastern equatorial Pacific sea surface temperature and rainfall over India and Sri Lanka. Mon. Wea. Rev. 111, 517-528 doi:10.1175/1520-0493(1983)111<0517:TRBEEP>2.0.CO;2

Rayner, N.A., Parker, D.E., Horton, E.B., Folland, C.K., Alexander, L.V., Rowell, D.P., Kent, E.C., Kaplan, A., 2003, Global analyses of sea surface temperature, sea ice, and night marine air temperature since the late nineteenth century. J. Geophys. Res., 108 D14, 4407 doi: 10.1029/2002JD002670

Reverdin, G., Cadet, D., Gutzler, D., 1986. Interannual displacements of convection and surface circulation over the equatorial Indian Ocean. Quart. J. Roy. Meteorol. Soc. 112, 43-46 doi: 10.1002/qj.49711247104

Sahu, N., Behera, S.K., Yamashiki, Y., Takara, K., Yamagata, T., 2012. IOD and ENSO impacts on the extreme stream-flows of Citarum river in Indonesia. Clim. Dyn. doi:10.1007/s00382-011-1158-2.

Saji, N.H., 2018. The Indian Ocean Dipole. Oxf Res Encycl Clim Sci doi : 10.1093/acref ore/97801 90228 620.013.619

Saji, N.H., Goswami, B.N., Vinaychandran, P.N., Yamagata, T., 1999. A dipole mode in the tropical Indian Ocean. Nature 401, 360-363 doi: 10.1038/43854

Santoso, A., England, M.H., Cai, W., 2012. Impact of Indo-Pacific feedback interactions on ENSO dynamics diagnosed using ensemble climate simulations. J. Clim. 25, 7743-7763 doi: 10.1175/JCLI-D-11-00287.1

Schott, F.A., Xie, S.-P., McCreary, J.P., 2009. Indian Ocean circulation and climate variability. Rev. Geophys. 47, RG1002 doi: 10.1029/2007rg000245

Shukla, R.P., Huang, B., 2016: Interannual variability of the Indian summer monsoon associated with the air–sea feedback in the northern Indian Ocean. Clim. Dyn. 46, 1977-1990 doi: 10.1007/s00382-015-2687-x

Sikka, D.R., 1980. Some aspects of the large-scale fluctuations of summer monsoon rainfall over India in relations to fluctuations in the planetary and regional scale circulation parameters. J. Earth Syst. Sci. 89, 179-195 doi: 10.1007/BF02913749

Slingo, J.M., Annamalai, H., 2000. 1997: The El Niño of the century and the response of the Indian summer monsoon. Mon. Wea. Rev. 128, 1778-1797 doi: 10.1175/1520-0493(2000)128<1778:TENOOT>2.0.CO;2

Sreejith, O.P., Panickal, S., Rajeevan, M., 2015. An Indian precursor for Indian summer monsoon rainfall variability. Geophys. Res. Lett. 42(21), 9345-9354 doi: 10.1002/2015GL065950

Srinivasan, J., Nanjundiah, R.S., 2002. The evolution of Indian summer monsoon in 1997 and 1983. Meteor. Atm. Phys. 79(3-4), 243-257 doi: 10.1007/s007030300006

Srivastava, A., Pradhan, M., Goswami, B.N., Rao, S.A., 2019. Regime shift of Indian summer monsoon rainfall to a persistent arid state: external forcing versus internal variability. Met. Atm. Phys. 131, 211-224 doi: 10.1007/s00703-017-0565-2

Stuecker, M.F., Timmermanss, A., Jin, F.F., Chikamoto, Y., Zhang, W., Wittenberg, A.T., Widiasih, E., Zhao, S., 2017. Revisiting ENSO/Indian Ocean dipole phase relationships. Geophys. Res. Lett. 44, 2481-2492 doi: 10.1002/2016GL072308

Taschetto, A.S., Ambrizzi, T., 2012. Can Indian Ocean SST anomalies influence South American rainfall? Clim. Dyn. 38, 1615-1628 doi: 10.1007/s00382-011-1165-3

Terray, P., Dominiak, S., Delecluse, P., 2005. Role of the southern Indian Ocean in the transitions of the monsoon-ENSO system during recent decades. Clim. Dyn. 24,169-195 doi: 10.1007/s00382-004-0480-3

Terray, P., Chauvin, F., Douville, H., 2007. Impact of southeast Indian Ocean sea surface temperature anomalies on monsoon-ENSO dipole variability in a coupled ocean-atmosphere model. Clim. Dyn. 28, 553-580 doi: 10.1007/s00382-006-0192-y

Terray, P., Kamala, K., Masson, S., Madec, G., Sahai, A.K., Luo, J.J., Yamagata, T., 2012. The role of the intra-daily SST variability in the Indian monsoon variability and monsoon-ENSO–IOD relationships in a global coupled model. Clim. Dyn. 39, 729-754 doi: 10.1007/s00382-011-1240-9

Terray, P., Masson, S., Prodhomme, C., Roxy, M.K., Sooraj, K.P., 2016. Impacts of Indian and Atlantic oceans on ENSO in a comprehensive modeling framework. Clim. Dyn. 46, 2507-2533 doi: 10.1007/s00382-015-2715-x

Ummenhofer, C.C., Schwarzkopf, F.U., Meyers, G.A., Behrens, E., Biastoch, A., Boning, C.W., 2013 Pacific Ocean contribution to the asymmetry in eastern Indian Ocean variability. J. Clim. 26, 1152-1171 doi: 10.1175/JCLI-D-11-00673.1

Ummenhofer, C.C., Sen Gupta, A., Briggs, P.R., England, M.H., McIntosh, P.C., Meyers, G.A., Pook, M.J., Raupach, M.R., Risbey, J.S., 2011. Indian and Pacific ocean influences on southeast Australian drought and soil moisture. J. Clim. 24, 1313-1336 doi: 10.1175/2010JCLI3475.1

Vecchi, G.A., Soden, B.J., Wittenberg, A.T., Held, I.M., Leetma, A., Harrison, M.J., 2006. Weakening of tropical Pacific atmospheric circulation due to anthropogenic forcing. Nature 441, 73-76 doi: 10.1038/nature04744

Walker, G.T., 1924. Correlation in seasonal variations of weather - A further study of world weather. Mon. Wea. Rev. doi: 10.1175/1520-0493(1925)53<252:CISVOW>2.0.CO;2

Wang, H., Murtugudde, R., Kumar, A., 2016: Evolution of Indian Ocean dipole and its forcing mechanisms in the absence of ENSO. Clim. Dyn. 47, 2481-2500 doi:10.1007/s00382-016-2977-y

Wang, H., Kumar, A., Murtugudde, R., Narapusetty, B., Seip, K., 2019. Covariations between the Indian Ocean dipole and ENSO: A modeling study. Clim. Dyn. 53, 5743-5761 doi: 10.1007/s00382-019-04895-x

Webster, P.J., Hoyos, C.D., 2010. Beyond the spring barrier? Nature Geosci. 3, 152-153 doi: 10.1038/ngeo800

Webster, P.J., Magana, V., Palmer, T.N., Shukla, J., Tomas, R.A., Yanai, M., Yasunari, T., 1998. Monsoons: processes, predictability and the prospects for prediction. J. Geophys. Res. 103, 14451-14510 doi: 10.1029/97JC02719

Webster, P.J., Moore, A.M., Loschnigg, J.P., Leben, R.R., 1999. Coupled ocean-atmosphere dynamics in the Indian Ocean during 1997-1998. Nature 401, 356-360 doi: 10.1038/43848

Weller, E., Cai, W., 2013. Asymmetry in the IOD and ENSO teleconnection in a CMIP5 model ensemble and its relevance to regional rainfall. J. Clim. 26(14), 5139-5149 doi: 10.1175/JCLI-D-12-00789.1

Wieners, C.E., Dijkstra, H.A., de Ruijter, W.P.M., 2017a. The influence of the Indian Ocean on ENSO stability and flavor. J. Clim. 30, 2601-2620 doi: 10.1175/JCLI-D-16-0516.1

Wieners, C.E., Dijkstra, H.A., de Ruijter, W.P.M., 2017b. The influence of atmospheric convection on the interaction between the Indian Ocean and ENSO. J. Clim. 30, 10155-10178 doi: 10.1175/JCLI-D-17-0081.1

Wittenberg, A.T., 2009. Are historical records sufficient to constrain ENSO simulations? Geophys. Res. Lett. 36, L12702 doi: 10.1029/2009GL038710

Wittenberg, A.T., Rosati, A., Delworth, T.L., Vecchi, G.A., Zeng, F., 2014. ENSO modulations: Is it decadally predictable? J. Clim. 27, 2667-2681 doi: 10.1175/JCLI-D-13-00577.1

Wu, R., Kirtman, B., 2004. Impact of the Indian Ocean on the Indian summer monsoon-ENSO relationship. J. Clim. 17, 3037-3054 doi: 10.1175/1520-0442(2004)017<3037:IOTIOO>2.0.CO;2

Xie, S.P., Annamalai, H., Schott, F.A., McCreary, J.P., 2002. Structure and mechanisms of south Indian Ocean climate variability. J. Clim. 15(8) 864-878 doi: 10.1175/1520-0442(2002)015<0864:SAMOSI>2.0.CO;2

Yamagata, T., Behera, S.K., Rao, S.A., Saji, N.H., 2003. Comments on "Dipoles, temperature gradients and tropical climate anomalies". Bull. Amer. Meteor. Soc. 84, 1418-1422

Yamagata, T., Behera, S.K., Luo, J.J., Masson, S., Jury, M.R., Rao, S.A., 2004. Coupled ocean-atmospheric variability in the tropical Indian Ocean. Earth Climate: The Ocean-Atmosphere Interaction, Geophys. Monogr. No. 147, American Geophysical Union, 189-212

Yang, J., Liu, Q., Xie, X.-P., Liu, Z., Wu, L., 2007. Impact of the Indian Ocean SST basin mode on the Asian summer monsoon. Geophys. Res. Lett. 34, L02708, doi:10.1029/2006GL028571.

Yuan, Y., Li, C.Y., 2008. Decadal variability of the IOD-ENSO relationship. Chin. Sci. Bull. 53, 1745-1752 doi: 10.1007/s11434-008-0196-6

Zhao, Y., Nigam, S., 2015. The Indian Ocean dipole: a monopole in SST. J. Clim. 28, 3-19 doi: 10.1175/JCLI-D-14-00047.1

Zhao, S., Jin, F.-F., Stuecker, M.F., 2019. Improved predictability of the Indian Ocean Dipole using seasonally modulated ENSO forcing forecasts. Geophys. Res. Lett. 46, 9980-9990 doi: 10.1029/2091GL084196

Zheng, X.T., Xie, S.P., Vecchi, G.A., Liu, Q., Hafner, J., 2010. Indian Ocean dipole response to global warming: Analysis of ocean-atmosphere feedbacks in a coupled model. J. Clim. 23, 1240-1253 doi: 10.1175/2009JCLI3326.1

Zheng, X.T., Xie, S.P., Du, Y., Liu, L., Huang, G., Liu, Q., 2013. Indian Ocean dipole response to global warming in the CMIP5 multi-model ensemble. J. Clim. 26, 6067-6080 doi:10.1175/JCLI-D-12-00638.1

Zhou, Q., Duan, W., Mu, M., Feng, R., 2015. Influence of positive and negative Indian Ocean dipoles on ENSO via the Indonesian throughflow: Results from sensitivity experiments. Adv. Atm. Sci. 32, 783-793 doi: 10.1007/s00376-014-4141-0

Zhou, T., Turner, A.G., Kinter, J.L., Wang, B., Qian, Y., Chen, X., Wu, B., Liu, B., Zou, L., He, B., 2016: GMMIP (v1.0) contribution to CMIP6: global monsoons model inter-comparison project. Geosci. Model Dev. 9, 3589-3604 doi: 10.5194/gmd-9-3589-2016

Zubair, L., Rao, S.A., Yamagata, T., 2003. Modulation of Sri Lankan Maha rainfall by the Indian Ocean Dipole. Geophys. Res. Lett. 30(2) doi: 10.1029/2002GL015639

Figure captions:

Fig. 8-1: Schematic of the Indian Ocean Dipole in its positive phase with warm SST anomalies on the west and cold SST anomalies toward the coast of Sumatra. The green arrows indicate the direction of the prevailing corresponding surface winds.

Fig. 8-2: Normalized monthly IOD index (std) defined as anomalous SST gradient between the western equatorial Indian Ocean (50°E-70°E and 10°S-10°N) and the southeastern equatorial Indian Ocean (90°E-110°E and 10°S-0°N). Anomalies have been downloaded from https://psl.noaa.gov/gcos_wgsp/Timeseries/DMI/, but 2019 values have been integrated from JAMSTEC repository (http://www.jamstec.go.jp/virtualearth/general/en/index.html). Red and blue markers along 6 and -6 std correspond to NINO3.4 anomalies (1981-2010 mean removed) larger than 0.5°C. NINO3.4 anomalies have been downloaded from https://psl.noaa.gov/gcos_wgsp/Timeseries/Nino34/. As indicated in the respective websites, both IOD and NINO3.4 values are computed from the HadISST1 dataset (Rayner et al., 2003).

Fig. 8-3: (a) Positive IOD composite of specific humidity (mm, shaded) and moisture flux (integrated up to 300 hPa, kg/m/s, vectors) anomalies averaged in summer (JJAS). The figure is taken from Behera and Ratnam (2018); (b) schematic of the IOD influence on ISM rainfall embedded in the TBO (adapted from the scheme in Webster and Hoyos (2010).

Fig. 8-4: June to September (a-d) rainfall (shading), 850-hPa wind (vectors), and (e-h) 200-hPa velocity potential anomalies regressed onto normalized boreal fall (i.e., SON) SST anomalies over the eastern IOD pole (domain: 90°E–110°E, 10°S–0°) when ENSO is removed. Significant anomalies at the 90% level are shown with black contours for rainfall and 200-hPa velocity potential anomalies, and with purple vectors for 850-hPa wind anomalies. Positive 200-hPa velocity potential anomalies correspond to abnormal upper-level mass flux convergence. Adapted from Cretat et al. (2017).

Fig. 8-5: 2019 case from (a) June to (d) September for SST (°C), 850 hPa winds (m/s) and precipitation (mm) anomalies with respect to 1980-2010 mean climatology. SST data is taken from ERSSTv5 (Huang et al. 2017), 850 hPa wind vectors are obtained from ECMWF ERA5 reanalysis (Hersbach and Dee, 2016) and precipitation from daily gridded rainfall dataset over India (Pai et al. 2014).

Fig. 8-6: (a) Monthly DMI index (anomalies, °C) for 20th and 21st centuries from a subset of CMIP6 models (Table 1). The index has been computed as in Fig. 2 (same areas difference and anomalies with respect to the 1980-2010 mean climatology). The index has been computed for each model and then averaged to obtain the ensemble mean. (b,c) SST (°C, shaded) and (d,e) precipitation (mm/day, shaded) and 850 hPa wind (m/s, vectors) regressed on the DMI index (values for 1°C change in the index) for JJAS mean during the historical period and the future projection, respectively. One member for each model has been considered. For the 21st century, the SSP5-8.5 scenario has been used. In panels c and e, the timeseries have been detrended before computing the regression, to keep out the trend from the related variability.